Structure and Properties of Amine-Hardened Epoxy/Benzoxazine Hybrids: Effect of Epoxy Resin Functionality

S. Grishchuk,[1] S. Schmitt,[1] O. C. Vorster,[2] J. Karger-Kocsis[2,3]

[1]*Institut für Verbundwerkstoffe GmbH (Institute for Composite Materials), Kaiserslautern University of Technology, D-67663 Kaiserslautern, Germany*
[2]*Polymer Technology, Faculty of Engineering and the Built Environment, Tshwane University of Technology, Pretoria 0001, Republic of South Africa*
[3]*Department of Polymer Engineering, Faculty of Mechanical Engineering, Budapest University of Technology and Economics, H-1111 Budapest, Hungary*

Received 22 March 2011; accepted 18 July 2011
DOI 10.1002/app.35302
Published online 3 November 2011 in Wiley Online Library (wileyonlinelibrary.com).

ABSTRACT: Bifunctional, trifunctional, and tetrafunctional epoxy resins (EP) were hardened with stoichiometric amount of 4,4′-diaminodiphenyl methane in presence and absence of benzoxazine (BOX). The EP/BOX ratio of the hybrid systems was 100/0, 75/25, 50/50, and 25/75 wt %, respectively. Information on the structure of the hybrid systems was received from differential scanning calorimetry, dynamic-mechanical thermal analysis, atomic force microscopy, and fractographic studies. The flexural and fracture mechanical properties of the EP/BOX hybrids were determined and compared to those of the reference EPs. The thermal degradation and fire resistance of the hybrids were also studied. It was found that the polymerized BOX was built in the network in from of nanoscale inclusions and acted as antiplasticizer. Incorporation of BOX enhanced the flexural modulus and strength and reduced the glass transition temperature of the parent EP. The fracture toughness and energy were practically not improved by hybridization with BOX. The charring and flame resistance were improved with increasing amount of BOX in the EP/BOX hybrids. The relative improvement in the latter was most prominent for the bifunctional EP/BOX systems. © 2011 Wiley Periodicals, Inc. J Appl Polym Sci 124: 2824–2837, 2012

Key words: thermoset; benzoxazine; epoxy resin; fracture mechanics; morphology

INTRODUCTION

Polybenzoxazines, formed by ring-opening polymerization of benzoxazine (BOX) precursors, are considered as promising matrix materials for composites in demanding applications. This expectation is based on their excellent thermal properties (high glass transition temperature, T_g), low flammability, high char yield, high stiffness, low water uptake, and practically no shrinkage upon curing.[1–4]. A further benefit is given by the synthesis of BOX, which may result in very versatile products. Among the disadvantages, the high polymerization temperature of BOX ($T > 200°C$), its outgassing and brittle behavior have to be mentioned. The development of BOXs addressed the above issues, except outgassing, in the past. Great efforts were devoted to find suitable catalysts[1,2,4] or novel BOX monomers[2,4,5] to reduce the polymerization temperature of BOX. The necessity of toughness improvement was also early recognized and the related work mostly followed the strategy proven for epoxy-based systems,[1,2,4,6] that is, to manipulate the crosslinked structure via cocrosslinking, and to incorporate or create a second, dispersed phase in the matrix.

Cocrosslinking of BOX with epoxy resins (EP) was always favored because the phenolic —OH groups of the ring-opened BOX could react with epoxy ones of EP, whereby the role of the EP curing agent was overtaken by the BOX.[1,2,4,7–12] EP/BOX[13] and EP/BOX/phenolic resin[14] combinations helped to reduce the outgassing, as well. However, the fracture mechanical performance could not be markedly improved by the EP/BOX combinations.[15,16]

In our companion work, we have investigated the structure-property relationships in various amine-cured bifunctional EPs modified with a fix amount of BOX.[16] This work considered the finding that primary diamines, being usual hardeners for EPs, may also react with BOX and accelerate the BOX homopolymerization at the same time.[16] The following reaction schema of BOX with primary amine has been proposed in the past[17,18] (see Scheme 1).

Correspondence to: J. Karger-Kocsis (karger@pt.bme.hu).
Contract grant sponsor: BMBF, Germany.
Contract grant sponsor: NRF, South Africa.
Contract grant sponsor: Hungarian Research Funds; contract grant number: OTKA NK 83421.
Contract grant sponsor: TIA, South Africa.

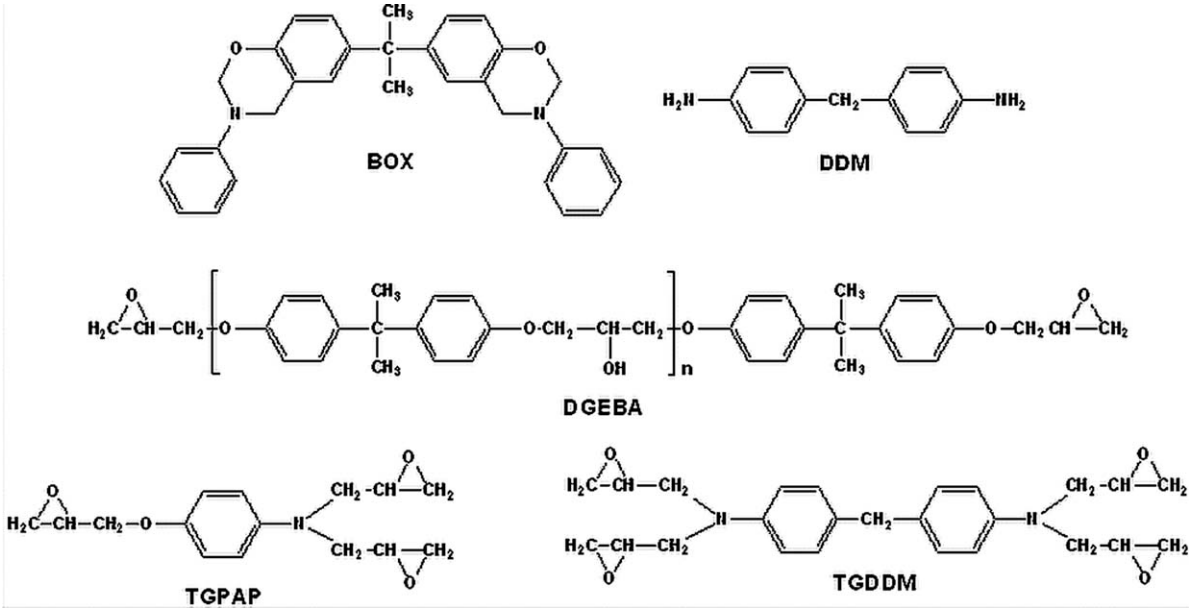

Figure 1 The chemical structures and abbreviations of the materials used.

The above reaction between BOX and primary amine yields a new hardener. This is also bifunctional as the primary amine, but bears different and less reactive functional groups (—OH and secondary amine). Nonetheless, the initial EP/amine stoichiometry does not change in this respect. By contrast, the EP/amine ratio does change with the homopolymerization of BOX owing to the phenolic —OH groups formed. It is known that off-stoichiometry may be accompanied with internal antiplasticization effect.[19] The aim of this work was to check whether such antiplasticization can be triggered in amine hardenable EP through hybridization with BOX. Accordingly, the structure and properties of aromatic diamine hardened EP/BOX resins as a function of BOX content (up to 75 wt %) and EP functionality (bifunctional, trifunctional, and tetrafunctional EPs) were determined and discussed.

EXPERIMENTAL

Materials

The chemical structures of the materials used are depicted in Figure 1. The BOX used was an *N*-phenyl bisphenol A based 1,3-bezoxazine (Araldite MT 35600 CH of Huntsman Advanced Materials, Basel, Switzerland). This BOX with a density of 1.18 g mL^{-1} at RT has a melting range of 80–85°C, and a viscosity range between 80 and 180 mPa s^{-1} at $T = 125$°C. It is noteworthy that this BOX grade is usually abbreviated by BA-a.

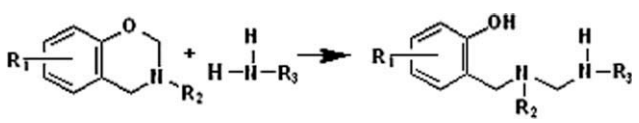

Scheme 1 Reaction between BOX and primary amine compound.

BOX was combined with EP resins of various functionalities. As bifunctional EP, a diglycidyl ether bisphenol A based one, namely D.E.R. 331 (Dow Deutschland Anlagengesellschaft mbH, Schwalbach, Germany) was selected. This EP, further referred as DGEBA, has the following characteristics: epoxy equivalent weight: 182–192 g eq^{-1}, viscosity and density at $T = 25$°C 11–14 Pa s^{-1} and 1.16 g mL^{-1}, respectively. The trifunctional aromatic EP was triglycidyl *p*-aminophenol (further on TGPAP), produced under the trade name Araldite MY 0510 by Huntsman Advanced Materials. Its epoxy equivalent weight was 95–106 g eq^{-1}, viscosity and density at $T = 25$°C were 550–850 mPa s^{-1} and 1.21 g mL^{-1}, respectively. The tetrafunctional EP, Araldite MY 721 also from Huntsman Advanced Materials, was tetraglycidyl diaminodiphenylmethane (further on TGDDM) with the following characteristics: epoxy equivalent weight: 109–116 g eq^{-1}, viscosity at $T = 50$°C; 3–6 Pa s^{-1}, and density at $T = 25$°C; 1.21 g mL^{-1}.

As EP hardener 4,4′-diaminodiphenyl methane (DDM) was chosen to ensure the compounds high glass transition temperature (T_g). DDM (melting temperature: 92°C) was procured from Sigma-Aldrich Chemie GmbH (Taufkirchen, Germany). It has to be underlined that DDM proved to be a weak accelerator of the BOX homopolymerization.[16]

Sample/specimen preparation

The samples were prepared as indicated below. First, the EP was warmed to 70°C and kept for

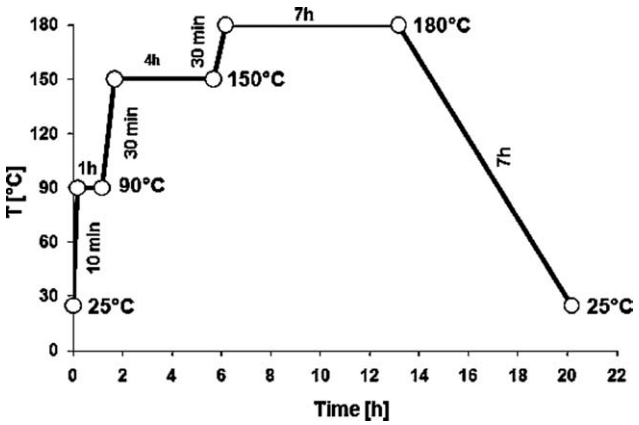

Figure 2 Cure cycle of the EP and EP/BOX hybrids.

30 min to melt the eventually crystalline fraction. Next, the powdered BOX was added to the warm EP and mixed through (1900 revolutions per minute, rpm) for 5 min. The mix was placed in a thermostatic oven and stored at $T = 120$°C for 40 min to dissolve the BOX. Afterwards, the amine was introduced by mixing (160 rpm) for 4 min. Finally, the mixture was deareated *in vacuo* and poured in open molds manufactured from polytetrafluoro ethylene (PTFE). The PTFE molds contained the cavities of the rectangular bars and compact tension (CT) specimens used for testing (see later).

The EP/amine ratio was stoichiometric in all recipes. Albeit the BOX reacts with both the amine compound and EP, as mentioned before, it was considered as an "inert" material in this work. The EP (including hardener)/BOX ratio was varied by setting 100/0, 75/25, 50/50, and 25/75 wt %, respectively, in the systems studied.

The cure cycle (temperature versus time) of the samples is depicted in Figure 2. Curing of the resins according to Figure 2 occurred in a programmable thermostatic oven of Kendro Laboratory Products (Langenselbold, Germany). The long holding time at $T = 180$°C was foreseen to achieve the complete curing of both EP and BOX. Note that EP/DDM systems are usually cured in the temperature range $T = 140 \ldots 180$°C. It was also demonstrated that the homopolymerization of BOX starts already at $T = 150$°C.[16]

Morphology determination

Morphology of the hybrid systems was studied by scanning electron and atomic force microscopy (SEM and AFM, respectively) techniques. The fracture surface of CT specimens (see later) was inspected in SEM using a JSM 5400 device of Jeol (Tokyo, Japan). The fracture surface was coated with an Au/Pd alloy prior to SEM inspection using a Balzers SCD 050 (Balzers, Lichtenstein) sputtering apparatus.

AFM scans were taken on polished samples by an AFM device (Veeco/Digital Instruments GmbH, Mannheim, Germany) in tapping mode, and the related height- and phase-contrast images captured. Commercial silicon cantilever (Pointprobe NCH of Nanosensors, Neuchatel, Switzerland) with a nominal tip radius of <10 nm (120 μm cantilever length, 4 μm thickness, 30 μm width, and spring constant at 42 Nm^{-1}, Nanosensors, Neuchatel, Switzerland) was employed under its fundamental resonance frequency of about 330 kHz. The scan rate was 0.5 Hz for all AFM images.

Thermal and viscoelastic properties

Differential scanning calorimetry (DSC 821e of Mettler Toledo, Giessen, Germany) was used to detect the T_g of the EP/BOX hybrids prepared. DSC thermograms were registered in the temperature range from $T = 0$ to 300°C at a heating rate of 10°C min^{-1} under N_2 flushing (30 mL min^{-1}). The sample weight varied between 10 and 20 mg.

Dynamic mechanical thermal analysis (DMTA) was taken on rectangular specimens (60 × 8 × 4 in mm; length × width × thickness) in three point bending configuration (span length: 50 mm) at 1 Hz using a DMA Q800 of TA Instruments (New Castle, DE). Tests were performed at a constant amplitude (50 μm) using sinusoidal oscillation and under dynamic conditions in the interval $T = -100 \ldots 300$°C at a heating rate of 1°C min^{-1}.

Flexural and fracture mechanical behavior

The flexural properties, namely, modulus and strength of the hybrid resins, were determined on rectangular specimens (60 × 8 × 4 in mm; length × width × thickness) in three point bending at room temperature according to EN63. The span length of the specimens was 50 mm and their loading on a Zwick 1474 (Zwick GmbH, Ulm, Germany) universal testing machine occurred with deformation rate $v = 1$ mm min^{-1}.

The fracture toughness (K_c) and fracture energy (G_c) were measured according to ISO 13586-1 standard. The tests were done on the Zwick 1445 machine at room temperature (RT) with a crosshead speed of $v = 1$ mm min^{-1}. The CT specimens (dimension: 35 × 35 × 3 in mm; length × width × thickness) were notched before loading by sawing. The sawn notch of the CT specimens was sharpened by a razor blade. The razor blade, fixed in a rig, was positioned in the notch root before hitting the fixing rig with a hammer. This "taping" yielded the desired sharp crack.

Thermogravimetric analysis and fire resistance

The hybrid resins were subjected to thermogravimetric analysis (TGA) in a DTG-60 device of Shimadzu

(Columbia, MD). The TGA experiments were conducted under nitrogen atmosphere (30 mL min^{-1}) in the temperature range $T = 25$–600°C with heating rate 10°C min^{-1}.

To test the fire resistance of the materials the UL 94V flammability vertical test[20] was chosen being a very stringent test. In the 94V flammability test, the specimen in vertical position is flamed from its bottom. The flame is applied for 10 seconds and then removed. The burning time is measured. Afterwards the flame is reapplied for another 10 seconds, and again the burning time is measured. The final classification of the materials (in our case, however, instead of five only three specimens of $\sim$ 4 mm thickness were tested for each formulation) depends on several parameters (e.g., burning time of the individual specimens, overall burning time of the three specimens, dropping caused burning of the cotton placed below the specimen). Classification of the samples into burning groups occurred using following criteria:

- Combustible: Specimens did burn with flaming combustion for more than 30 s after each flame application; total flaming combustion time did exceed 150 s for each of the three specimens; specimens did burn with flaming or glowing combustion up to the specimen-holding clamp; specimens experienced glowing combustion longer than 60 s after removal of the test flame.
- V-2: Specimens did not burn with flaming combustion for more than 30 s after each flame application; total flaming combustion time did not exceed 150 s for each of the three specimens; specimens did not burn with flaming or glowing combustion up to the specimen holding clamp; specimens produced flaming particles that ignited the cotton by dripping; no specimen had glowing combustion longer than 60 s after removal of the test flame.
- V-1: Specimens did not burn with flaming combustion for more than 30 s after each flame application; total flaming combustion time did not exceed 150 s for each of the three specimens; specimens did not burn with flaming or glowing combustion up to the specimen holding clamp; specimens did not drip flaming particles that ignited the cotton; no specimen had glowing combustion longer than 60 s after removal of the test flame.
- V-0: Specimens did not burn with flaming combustion for more than 10 s after each test flame application; total flaming combustion time did not exceed 30 s for each of the three specimens; specimens did not burn with flaming or glowing combustion up to the specimen holding clamp; specimens did not drip flaming particles that ignited the cotton; no specimen had glowing combustion longer than 30 s after removal of the test flame.

RESULTS AND DISCUSSION

Morphology of the EP/BOX hybrids

Figure 3 displays SEM pictures taken from the fracture surfaces of the bifunctional, trifunctional, and tetrafunctional EPs combined with BOX in 50/50 wt % ratio. Only these pictures have been selected to show some basic differences in the related systems. One can see that the roughness of the fracture surfaces of the EP/BOX hybrids decreases strongly with increasing functionality of the EP resin. This is the first hint that the fracture toughness and energy values decrease with increasing EP functionality. In DGEBA/BOX, a well-developed plastic zone can be resolved at the notch tip. This is less developed in TGPAP/BOX, and even less in TGDDM/BOX (cf. Fig. 3). High magnification SEM pictures from this region display the appearance of characteristic river-like patterns. It is well accepted in the literature that the larger and the rougher the plastic zone the higher the fracture toughness and energy values are. This will be proved later.

The fracture surface became smoother also with increasing amount of BOX in the related hybrid formulations, which is demonstrated on the example of DGEBA/BOX systems in Figure 4. A further interesting aspect is that no separate BOX phase could be resolved in Figures 3 and 4. This means that either EP or BOX are copolymerized, or the homopolymerized BOX is nanoscale dispersed, or both copolymerized fractions and phase segregated nanodomains are present at the same time in the EP. The latter assumption will be confirmed later by AFM results.

To get a deeper insight into the EP/BOX matrix morphology the EP/BOX systems were subjected to AFM inspection. AFM height and phase contrast images, taken from the polished surfaces of the DGEBA/BOX, TGPAP/BOX, and TGDDM/BOX at 50/50 weight ratio, are displayed in Figures 5(a–c), respectively. The white spots in the AFM phase images represent the polymerized BOX. The BOX, which is likely homopolymerized, is dispersed in submicron-scale domains in the EP matrix of the EP/BOX hybrids (cf. Fig. 5). This is in line with our previous results.[16] Apart of this phase-segregated one, a homogeneously cocrosslinked EP-BOX phase should also be present. The difference in the BOX dispersion as a function of the EP functionality reflects that the final shape and size of the domains are governed by the interplay between chemorheology and phase segregation kinetics. However, there is still an open question whether or not the BOX is fully polymerized. To check this issue, AFM work

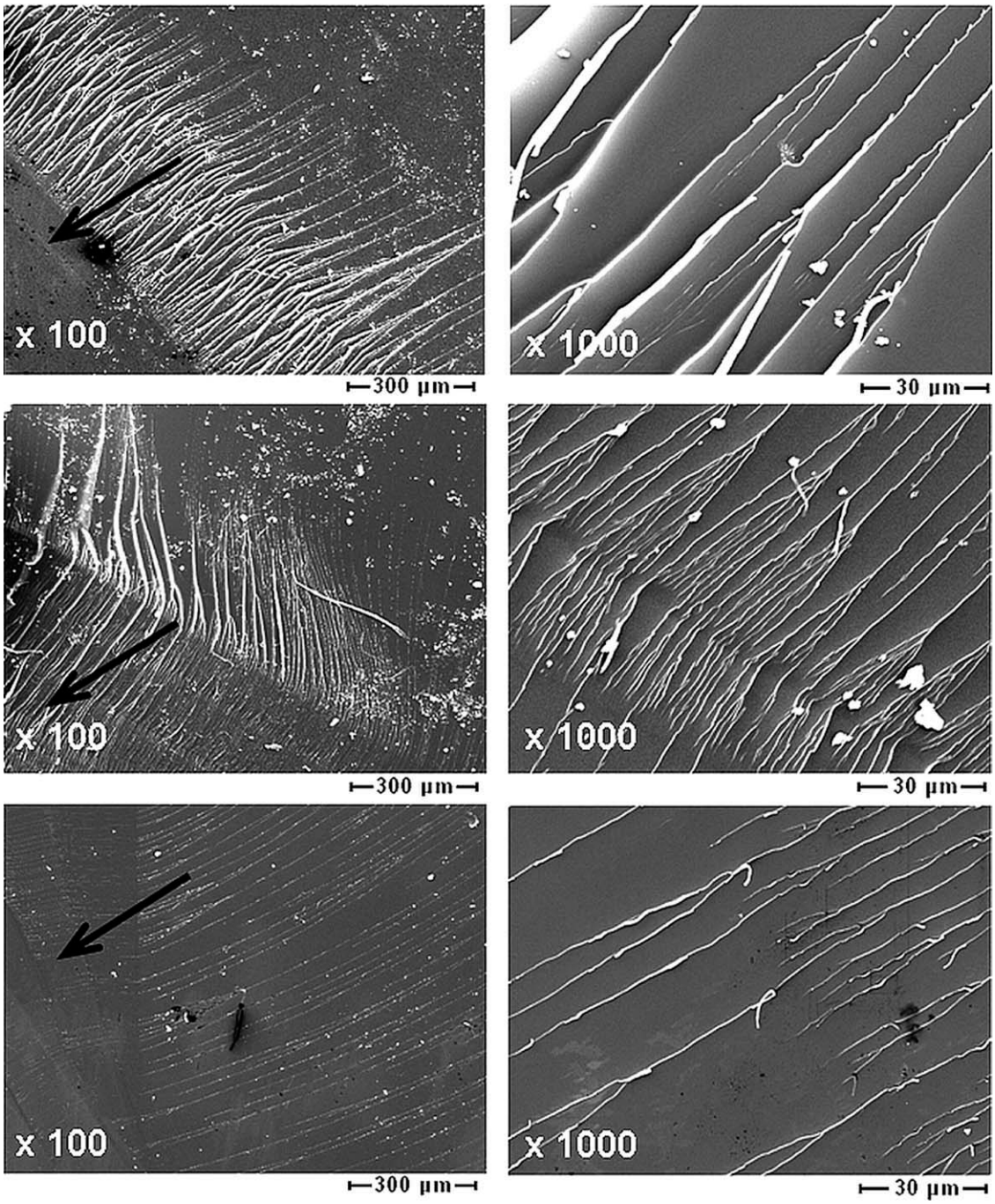

Figure 3 SEM pictures at different magnifications taken from the fracture surfaces of DGEBA/BOX (top), TGPAP/BOX (middle), and TGDDM/BOX (bottom) 50/50 wt % hybrids. Note: razor notching is indicated by arrow.

was done on polished specimens after etching them in acetone for 35 min followed by drying in vacuum oven for 5 h (to recover the shape of swollen EP matrix). Note that the acetone should solve the unpolymerized BOX very quickly. It was found, however, that acetone etching did not change the morphology and thus the white inclusions in the AFM images represent the polymerized BOX, in fact. It is straightforward to underline here that the combination of EP with BOX results in nanophase separation: the homopolymerized BOX becomes nanoscale dispersed in the EP.

Based on the AFM results the question arises: why the presence of polymerized BOX was not detected in DSC and DMTA results? This is due to overlapping of the T_g transitions of EP and polymerized BOX and postcuring phenomena taking place above the T_g.

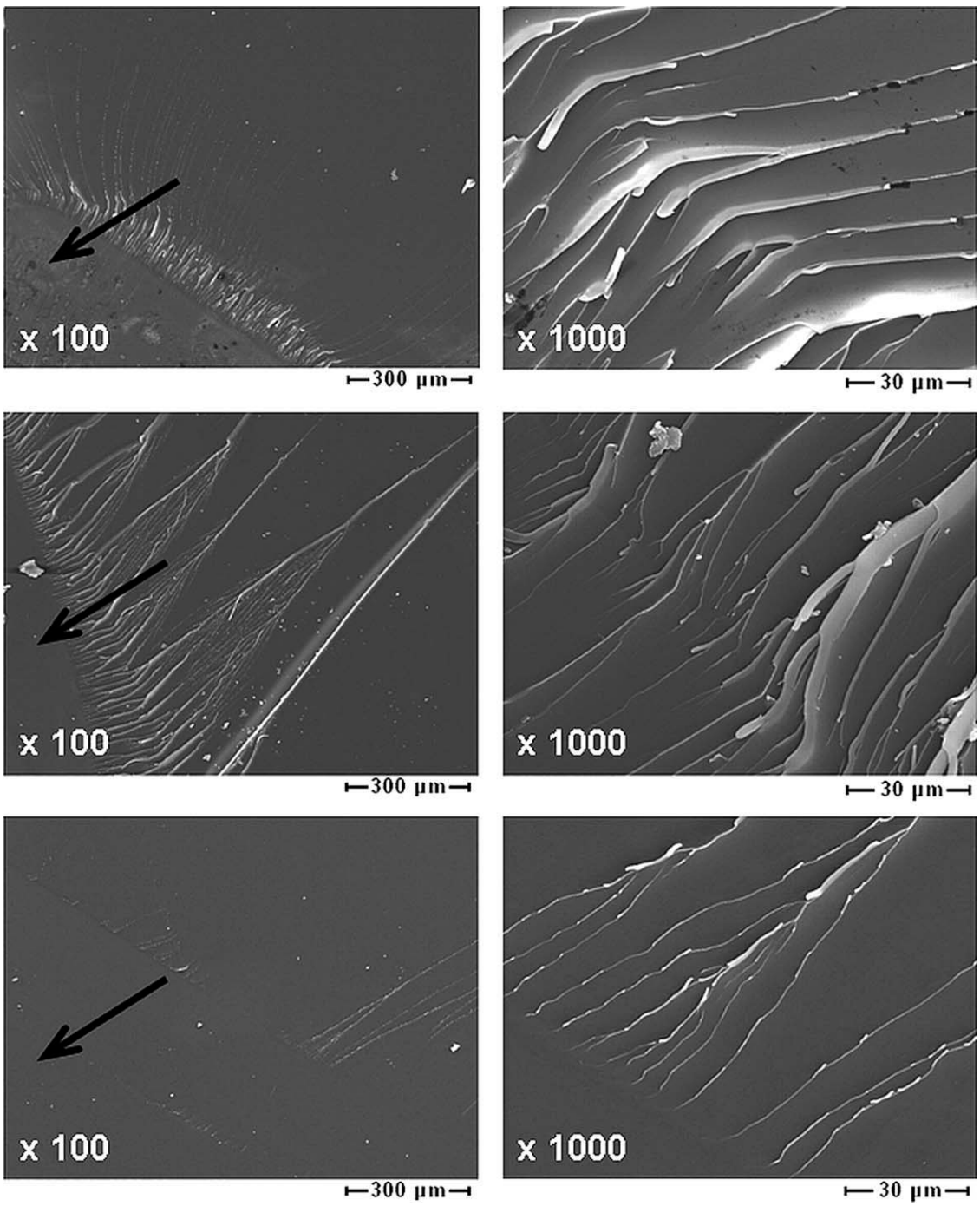

Figure 4 SEM pictures at different magnifications taken from the fracture surfaces of DGEBA (top), DGEBA/BOX = 75/25 wt % (middle), and DGEBA/BOX = 25/75 wt % hybrids (bottom). Note: razor notching is indicated by arrow.

Thermal and viscoelastic properties of EP/BOX hybrids

The T_g values, read from the DSC scans, are listed in Table I. In all cases, hybridization with BOX was associated with a shift in the T_g toward lower temperatures compared to the reference EPs. This is illustrated on the example of EP/BOX = 50/50 wt % hybrids based on the EPs of different functionalities in Figure 6. The observed shift in the T_g values is due to the EP/BOX network structure, which differs from that of the initial EP owing to coreactions of both the EP and amine hardener with the BOX. A similar shift in the T_g was found in our companion work dealing with DGEBA/BOX systems.[16] The related T_g shift became more prominent with increasing functionality of the EP used (cf. Table I). The T_g values of EP/BOX hybrids with trifunctional and tetrafunctional EPs were reduced with

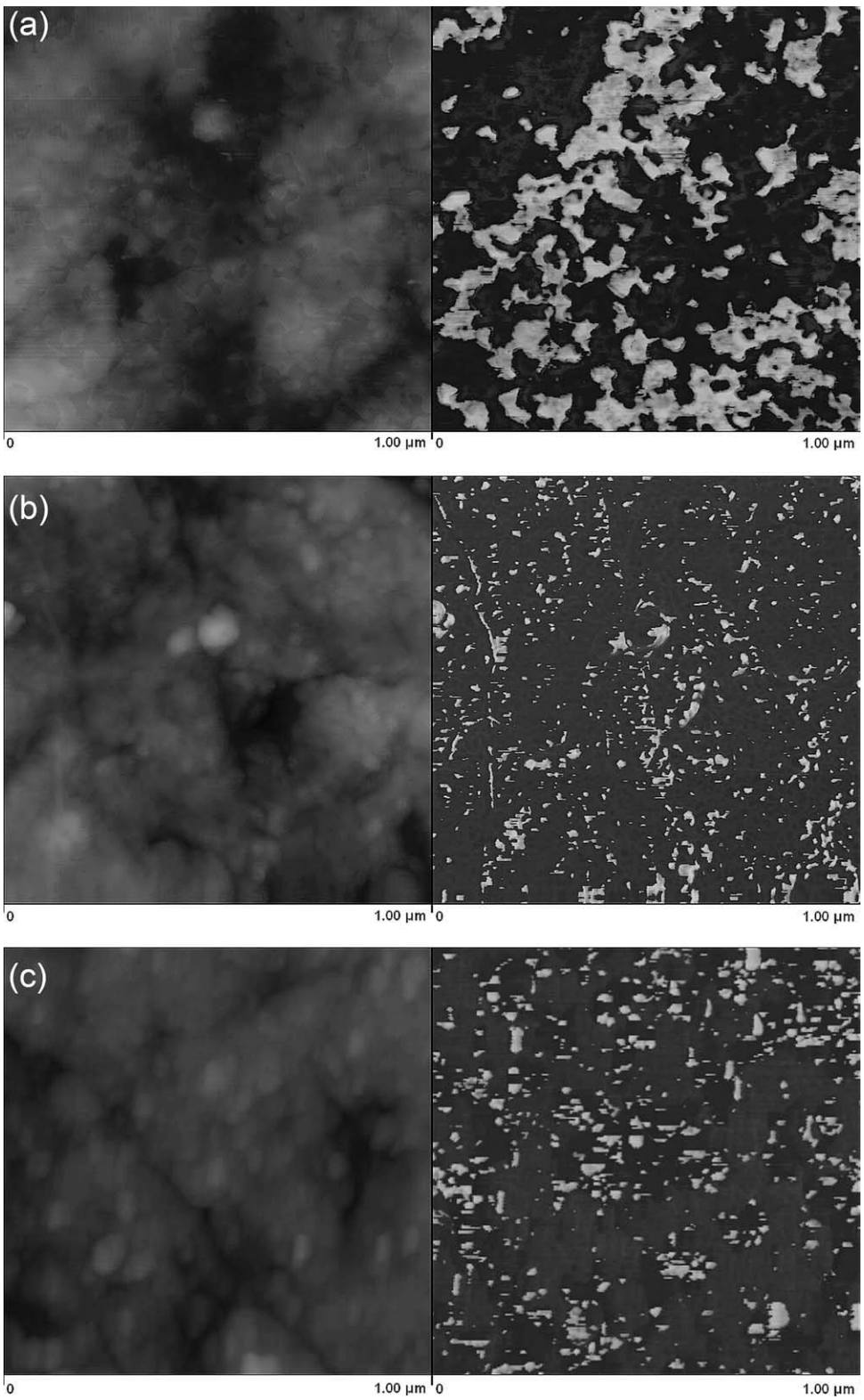

Figure 5 (a) AFM height (left) and phase images (right) taken from the polished surface of DGEBA/BOX = 50/50 wt %. (b) AFM height (left) and phase images (right) taken from the polished surface of TGPAP/BOX = 50/50 wt %. (c) AFM height (left) and phase images (right) taken from the polished surface of TGDDM/BOX = 50/50 wt %. Note: pictures a to c from the top to the bottom.

increasing amount of BOX, as well. By contrast, an increase in T_g values was observed with increasing amount of BOX for the DGEBA/BOX based systems (cf. Table I; Fig. 7). This is probably due to differences in T_g values of the parent EPs compared to that of polymerized BOX (the T_g of this polymerized

TABLE I
T_g and Selected DMTA and TGA Parameters of the Resin Combinations Studied

System	T_g (°C)		E' (MPa)		ν_c (mol dm^{-3})	$T_{5\%}$ (°C)	Char yield at $T = 600$°C (wt %)
	DSC	DMTA	RT	$T_g + 30$°C			
DGEBA-Ref	170	174	2627	43	3.61	372	18
DGEBA/BOX = 75/25 wt %	160	164	3725	30	2.58	355	22
DGEBA/BOX = 50/50 wt %	162	173	4200	30	2.53	346	27
DGEBA/BOX = 25/75 wt %	165	183	4405	30	2.47	342	30
TGPAP-Ref	>210[a]	240	3841	84	6.20	325	27
TGPAP/BOX = 75/25 wt %	187	210	4040	91	7.11	324	29
TGPAP/BOX = 50/50 wt %	175	191	4436	55	4.46	328	28
TGPAP/BOX = 25/75 wt %	172	183	5916	47	3.88	330	29
TGDDM-Ref	>210[a]	253	3680	59	4.25	329	26
TGDDM/BOX = 75/25 wt %	>200[a]	226	4022	82	6.21	332	26
TGDDM/BOX = 50/50 wt %	196	206	4508	59	4.65	335	25
TGDDM/BOX = 25/75 wt %	175	190	3985	37	3.01	329	28

[a] Difficult to resolve because of strong overlapping with the post-curing exothermic peak.

BOX is about $T = 170$ and $T = 180$°C based on DSC and DMTA results, respectively). Major source of the T_g reduction is the fact that the crosslink density of the polymerized BOX is below that of the neat EP, at least for TGPAP and TGDDM.

It should be also mentioned that some postcuring effects (exothermic peak after the glass transition region) were observed for the neat EP and EP/BOX hybrids. These effects become more prominent with increasing functionality of EPs (cf. Fig. 6) and increasing amount of BOX (Fig. 7). However, it is important to note that postcuring exotherms of the reference EPs are strongly reduced by incorporation of BOX, and especially for the EPs of higher functionality (cf. Fig. 6). This fact indicates that the conversion of all functional groups (epoxy, amine, oxazine, and secondary hydroxyls) increases due to coreactions with BOX during curing, and suggests that BOX is chemically bonded to the EP-components. Moreover, increasing functionality of the EP resins supports the cocrosslinking reactions with BOX. This is likely because the reactivity of EP increases with its increasing functionality. Note that the initial amine/oxazine and epoxy/oxazine ratios all increase with EP-functionality in the hybrids, whereas the amine/epoxy ratio remained stoichiometric. This contributes to reactions between oxazine (BOX) and amine (DDM) groups and between phenolic hydroxyls (BOX) and epoxy groups (EP) during curing. Further, the position of T_g in respect to the temperature of the final curing step (viz., 180°C.; cf. Fig. 2) should also be taken in account. If the curing temperature (T_{cure}) is higher than the T_g, or T_{cure} is close to the T_g of the related system, a higher conversion of the functional groups is expected than for $T_{cure} < T_g$. Because most of EP/BOX hybrids have a T_g, lower or comparable with T_{cure}, they exhibit limited postcuring effects. The DSC-related T_g data in Table I indicate that hybridization with increasing amount of BOX reduced the T_g of EP, that is, plasticization took place as expected. However, the DGEBA/BOX hybrids do not follow this trend. This may be linked with the difference in the T_g data of EP and

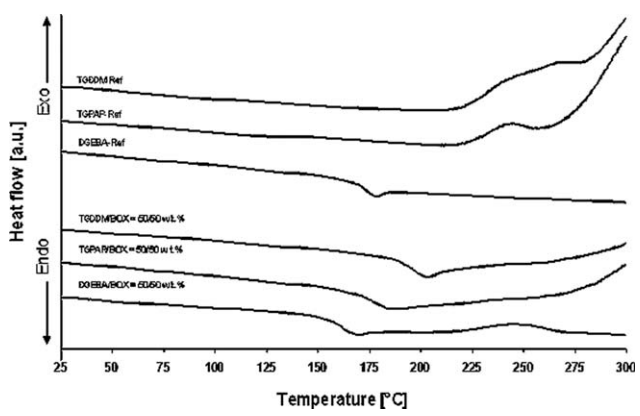

Figure 6 DSC thermograms registered for the EPs and their EP/BOX = 50/50 wt % hybrids.

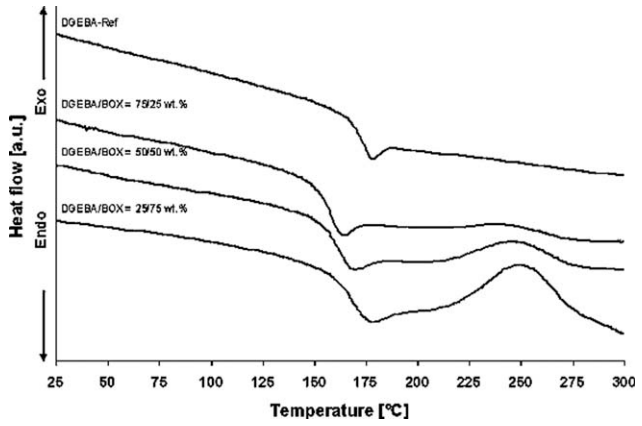

Figure 7 DSC thermograms registered for the DGEBA-Ref and its EP/BOX hybrids.

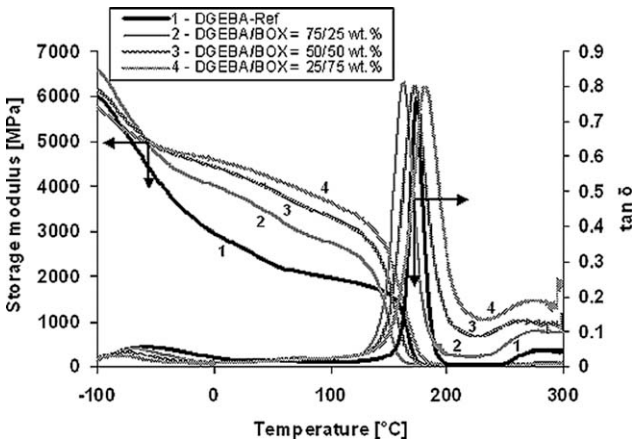

Figure 8 Storage modulus (E') and mechanical loss factor (tan δ) as a function of temperature for the DGEBA-Ref and DGEBA/BOX hybrids.

homopolymerized BOX (the latter is higher), which influences the curing in the regime adapted (cf. Fig. 2). Moreover, also the relative amount of BOX in the corresponding hybrid affects the T_g.

The DSC results were confirmed by the DMTA results. The temperature dependences of storage modulus (E') and loss factor (tan δ) as function of EP/BOX ratio are presented on the example of DGEBA and TGPAP based hybrids in Figures 8 and 9. The DMTA traces of the TGDDM-based systems are very similar to those of TGPAP/BOX hybrids, except that the T_g values are slightly higher for the former and some differences exist in the storage moduli at room temperature (RT; cf. Table I). Therefore, they are not presented here. In general, one single T_g was detected for all EP/BOX hybrids. This indicates a high level of component compatibility for the EP/BOX hybrids. Good compatibility is likely given by the similar nature (aromatic) of EP and BOX, and coreactions (grafting) between the EP and BOX networks, resulting in a hybrid structure.

The plateau moduli in the rubbery stage (E'_R) were read at T_g + 30°C for the EP and EP/BOX hybrids studied, and are also listed in Table I. These E'_R data were used to estimate the apparent crosslink density according the theory of rubber elasticity:

$$\upsilon_c = E'_R/(3RT) \quad (1)$$

where υ_c is the crosslink density, R is the gas constant, and T is the absolute temperature (i.e., at T_g + 30°C).

Although not fully correct, the theory of rubber elasticity is very frequently adapted for EP-based systems and the crosslinking density deduced is termed "apparent." Researchers dealing with various BOX polymers rather prefer the Nielsen equation to calculate the apparent crosslink density[21] (this was not followed, however, in this work). The plateau modulus might have been affected by postcuring effects, and in addition, it was read from one single DMTA trace. This is likely the reason why we have the expected trend, namely, T_g enhancement with increasing crosslink density, with some scattering, see data in Table I.

The T_g values, read as the peak temperatures of the α-relaxation transitions in the tan δ versus T traces, are also listed in Table I. The tan δ-T traces exhibit further peaks: γ- and/or β-relaxation peak in the low-temperature region, a low-intensity peak between the β- and α-transitions, and a peak linked with postcuring at $T > 220$°C.

The influence of BOX-content on the DMTA properties of the related hybrids was different for the bifunctional and multifunctional EPs. The E' versus T traces of DGEBA/BOX show that the homopolymerized and copolymerized BOX works as reinforcement in the EP (cf. Fig. 8). With increasing BOX content the E' versus T traces in the region between β- and α-relaxation transitions are shifted toward higher E' (stiffness) values. This is well documented by the E' values, read at room temperature (RT), in Table I. At the same time, the T_g is slightly reduced, at least up to 50 wt % BOX content. However, above this BOX threshold the T_g values increased again. This finding is in a good agreement with DSC data (cf. Fig. 7 and Table I). The T_g peak intensity did not change significantly with BOX hybridization. It became, however, broader with increasing amount of BOX indicating that a wider range of segmental units takes part in the α-relaxation process. This is probably caused by an increased amount of partially reacted molecular fragments and by a prominent heterogeneity of the hybrid networks formed. Similar broadening in the α-relaxation peak and a T_g increase with increasing amount of BOX has been

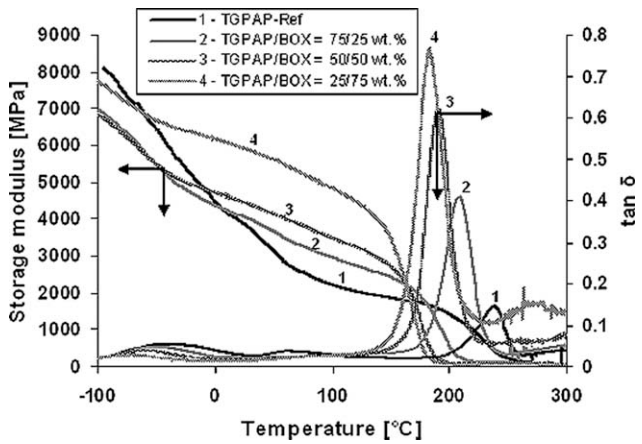

Figure 9 Storage modulus (E') and mechanical loss factor (tan δ) as a function of temperature for the TGPAP-Ref and TGPAP/BOX hybrids.

reported for BOX-containing EP.[22] Postcuring effects in the range $T > 220°C$ became also more obvious (cf. Figs. 8 and 9) with increasing amount of BOX, agreeing well with DSC data. Increasing intensity of tan δ versus T curves in this postcuring region suggests a lower conversion of functional groups with increasing amount of BOX. This is accompanied with reduced crosslink density as shown by the data in Table I.

Maintained T_g-peak intensity could be explained by the assumption that the effect of lower conversion of functional groups is compensated by the formation of novel network structure of lower free volume. This explanation seems to be supported by T_g increase with increasing in amount of BOX in the related DGEBA/BOX hybrids. Moreover, this assumption is straightforward based on two other aspects. First, the chemical build-up of DGEBA (bisphenol A backbone) and BOX are similar. Second, redistribution in the hydrogen bonds can strongly influence the properties (T_g, free volume) of polymeric systems. Recall that a high amount of hydrogen bonds is responsible for the high T_g of polymerized BOX resins, although this is associated with relative low crosslink density and low free volume.[2,23,24]

The scenario is somewhat different for the EP/BOX systems with higher EP functionalities, this is demonstrated on the example of TGPAP/BOX hybrids in Figure 9. Similar to DGEBA/BOX the BOX phase acts as reinforcement also in TGPAP/BOX (and in TGDDM/BOX–not shown here) as with increasing BOX amount the stiffness in the region between β- and α-transitions monotonously increases. Parallel to that, however, the T_g is monotonously decreasing. Note that this behavior is characteristics for antiplasticized EP systems.[25–27] The T_g shift toward lower temperatures is accompanied with the increasing intensity and broadening of the T_g peak. This suggests that with increasing BOX amount lower crosslink density of hybrid networks and broader distribution of relaxing segments are realized. This is well supported again by the corresponding data in Table I.

However, the crosslink density of EP/BOX systems containing fewer BOX is higher than that of reference EPs (cf. Table I). This can be explained by formation of cocrosslinked hybrid network structure different from that of the initial EP. Note that the probability of "hybrid interactions" between BOX- and EP-network decreases with increasing amount of BOX due to the reduction in amine/oxazine and oxirane/oxazine ratios (as discussed when interpreting the DSC results). By contrast, higher amount of hybrid interactions in hybrids containing less BOX should yield additional cocrosslinking sites resulting in higher crosslink density.

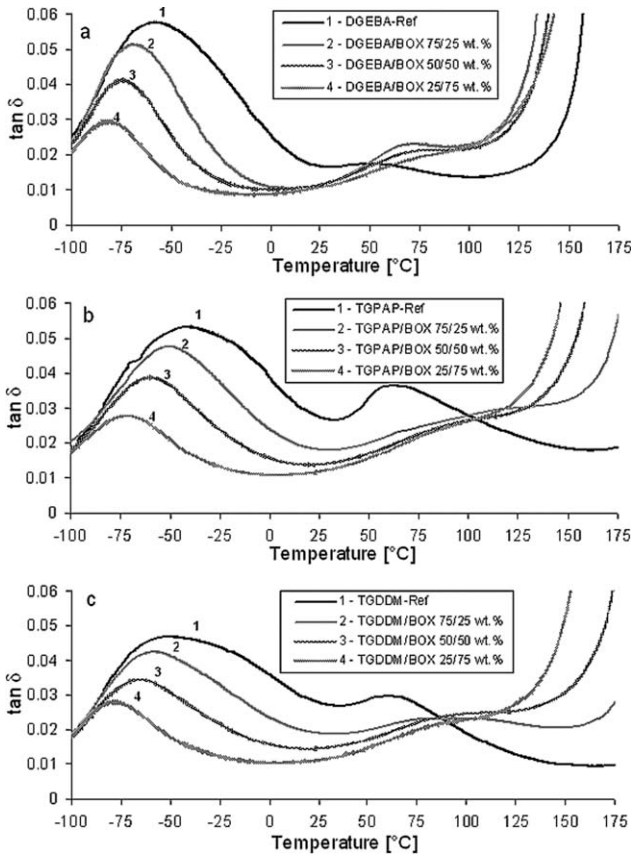

Figure 10 Mechanical loss factor (tan δ) as a function of temperature for the parent EPs and their EP/BOX hybrids.

The DMTA curves show further characteristics of antiplasticized systems, namely changes in the sub-T_g relaxation processes. In this context, the interest is usually devoted to the β-relaxation process, and thus we are focusing on this issue next.

The characteristic for DGEBA-Ref β-relaxation peak at $T = -55°C$ shifted toward lower temperatures and became narrower and less intensive with hybridization and increasing in amount of BOX [Fig. 10(a)]. Hybridization with BOX is accompanied also with a shift of the intermediate relaxation in sub-T_g region (i.e., between the α- and β-transitions) toward higher temperatures and with the onset of the α-transition at lower temperatures (antiplasticization). The intensity of this intermediate transition decreases with increasing in amount of BOX (cf. Fig. 10).

The mechanism of β-relaxation in polymers, including EP systems is not yet fully understood and controversially discussed in the literature. This is because of many factors that should be taken into account during interpretation. For example, size of relaxing groups,[28] size and position of substituents, stereochemical microstructures, stoichiometry,[29–31] curing procedure,[32] hydrothermal and physical ageing,[33,34] additives (either plasticizers or antiplasticizers),[25–27,35] etc. can influence the position and

intensity of β-relaxation. However, it is obvious that β-transition corresponds to relaxation motions of small moieties and their associates, which are much smaller than the chain segments. According to the literature, the β-relaxation of EPs (at $\sim -60°C$) is associated with crankshaft rotation of the hydroxyl ether structural units (—CH_2—CH(OH)—CH_2—O—). This is often overlapped with the β-relaxation of aromatic moities (for example, diphenylpropane units in case of DGEBA at $\sim -30°C$), which is usually accompanied with an additional intermediate relaxation in the region between β- and α-relaxation transitions.[27,31,36]

For polymerized bisphenol-based BOX resins in addition to the main α-relaxation process relaxation in the region of $\sim -70°C$ (termed as γ-relaxation) and intermediate relaxation in sub-T_g region (termed as β-relaxation) have been reported.[28,37,38] The motion of pendant groups in the Mannich bridges (attached to the nitrogen atoms) and movements within the Mannich bridges itself were found to be responsible for the above-mentioned low- and mid-temperature relaxation processes, respectively.[28]

Taking into account all of the above, decrease of intensity of the β-relaxation peaks in EP/BOX hybrids and their shifts to lower temperatures with increasing in BOX-content could be traced to several factors. First, the concentration of hydroxyl ether units is reduced with decreasing amount of the EP component in the hybrids. Therefore, the intensity of the β-relaxation at about $T = -55°C$ should be reduced. However, at the same time an increasing intensity in the γ-relaxation process of the BOX (pendant phenyl groups in the Mannich bridges) should be detected. However, it is not the case here that could be explained as follows. It is obvious that the β-relaxation of EPs (hydroxyl ether and aromatic units) is continuously disappearing with increasing BOX-content and becoming more similar to γ-relaxation of the homopolymerized BOX. In our opinion, it should be linked with hindrances of the movements of the EP β-relaxation-causing units due to additional chemical and physical interactions (e.g., hydrogen bonds). It was found that —OH···N hydrogen bonds are stable over the temperature range (50–190°C in the case of bisphenol A based polymerized BOX, that was used in this study) and are responsible for the β-relaxation in sub-T_g region of polymerized BOX. Opposite to this —OH···O hydrogen bonds are more temperature sensitive and their intensity is decreasing at the β-relaxation of polymerized BOXs.[23]

If only hydrogen bonds and their redistribution between the Mannich bases, hydroxyl ether fragments and phenolics (have more acidic character compare to the aliphatic alcohols) in EP/BOX hybrids are responsible for such stronger interactions, then an increased intensity in the intermediate relaxation process should be observed. This is, however, the case only for DGEBA/BOX. At the same time the characteristic β-relaxation of EP is reduced with increasing BOX content. The intensity of the intermediate relaxation peak decreased with increasing amount of BOX and increasing EP-functionality. According to Ning and Ishida[37], this is concerned with improved curing conditions. This is in good accordance with our assumptions, made in the discussion of DSC results above, considering more complete reaction when curing above T_g. Therefore, a higher level of chemical interactions (involving those units, which are responsible for the β-relaxation) should be the most important mechanisms along with the formation of strong hydrogen bonding in EP/BOX hybrids. By this way, the rotation of hydroxyl ether groups may be hindered due to chemical interaction between the secondary hydroxyls and phenolics (etherification), which is highly possible at high temperatures. This affects the α-relaxation, which broadens with increasing BOX content (cf. Figs. 8 and 9). It is far more difficult to explain the reduction of the β-relaxation linked with the aromatic groups in the EP-structures (being superimposed to the γ-relaxation of BOX). Many authors reported that BOX resins undergo secondary crosslinking reactions during polymerization (especially at higher postcuring temperatures). During this secondary crosslinking additional methylene-bridged structures form by the reaction of phenolic moieties in ortho and meta positions, and all positions of the arylamine rings.[2,39–41] It is known that curing of BOX resins occurs preferably through the formation of Mannich bridges in ortho and in lesser extent in para positions in respect to the phenolics hydroxyl group.[39,42] However, this is strongly obstructed by hydrogen bonds in case of para-substituted phenol-based BOXs.[43] However, very similar changes in the β-relaxation process were observed in EP networks modified with antiplasticizers (also termed as "fortifiers").[25,44,45] Antiplasticizers act usually via strong interactions with the polymer matrix, enhancing the strength and modulus of the respective material.[46] Antiplasticizing (i.e., a decrease in free volume, which restricts molecular mobility and hence increases the modulus[31,45]) is characterized by simultaneous enhancement of stiffness and reduction of T_g. This is usually accompanied with decreasing intensity of the β-relaxation process and reduction of the loss modulus in this region.[25,27] The phenomenon, termed "internal antiplasticization," is also known for thermosets and it was observed for example in nonstoichiometric or partially reacted EPs.[19,29] Internal antiplasticization is usually accompanied with decreasing storage modulus in the temperature range of β-relaxation, enhanced storage modulus in

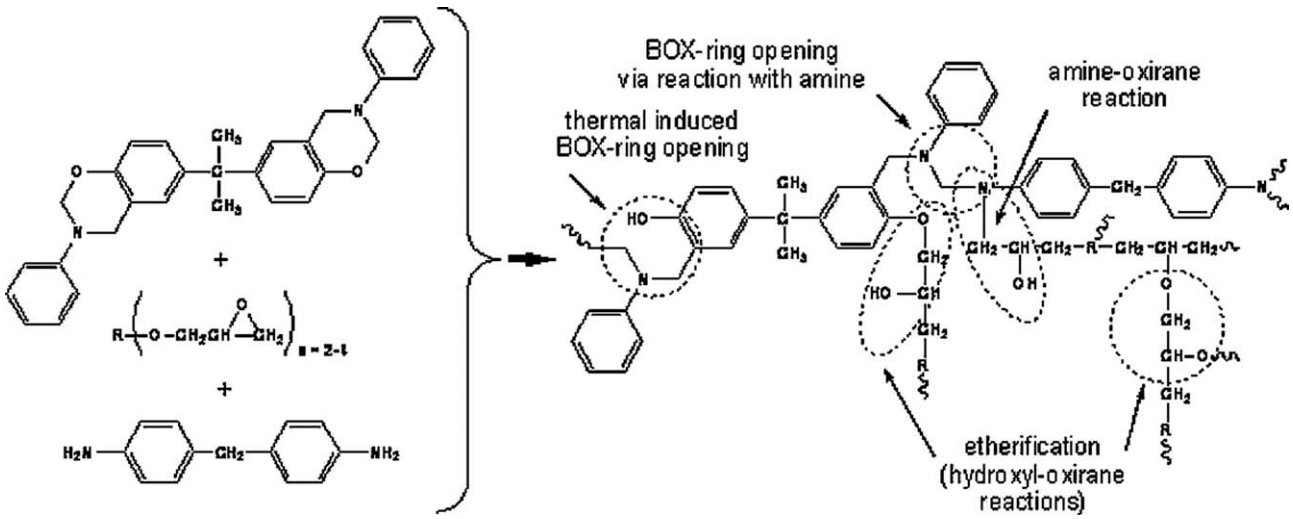

Figure 11 Chemical pathway of BOX-epoxy-amine cocuring reactions schematically. Note: R represented respective cores of EPs (viz., DGEBA, TGPAP, and TGDDM, respectively, see Fig. 1).

the region between β- and α-transitions, and reduced T_g. Moreover, the intensity of β-relaxation process decreases if the ratio amine/epoxy smaller than the stoichiometric one.[47] The inverse dependence of modulus on the degree of polymerization has been described as an indicator for internal antiplasticization, as well.[26,28,42] Similar antiplasticizing effect (shift of β-transition peak towards lower temperatures and lowering its intensity by an excess of epoxy prepolymer) has been attributed to the intermolecular hydrogen bonds between the unreacted epoxy groups and the relaxing units.[30] One can conclude that all above-mentioned effects are linked with changes in the network structure. The chemical reactions affecting the formation of the final network are summarized schematically in Figure 11. The related scheme, however, does not show the possible physical interactions (H-bonding).

To sum up, the major cause of internal antiplasticization is that the EP/DDM ratio is no more stoichiometric due to the reaction between the phenolic —OH of the homopolymerized BOX and epoxy groups. Recall that the oxazine(BOX)-amine(DDM) reaction generates an EP hardener which is still bifunctional but bears chemical groups of different reactivity compared to DDM.

In general, a decrease of intensity of both β- and α-transitions, and an increase of that for intermediate relaxation process were detected with increasing in EP functionality for the EP/BOX hybrids (cf. Fig. 10).

The DMTA analysis revealed that the modification of EP with BOX enhanced the stiffness (E-modulus), decreased the crosslink density and reduced the T_g. The decreasing crosslink density of the hybrids can be traced to the low crosslinking density of the homopolymerized BOX and to the off-

TABLE II
Flexural and Fracture Mechanical Data for the EPs and EP/BOX Hybrids

	Properties				
	Flexure			Fracture mechanics	
System	E_f (MPa)	σ_f (MPa)	ε_f (%)	K_c (MPa $m^{1/2}$)	G_c (J m^2)
DGEBA-Ref	2423 ± 257	122 ± 9	8.41 ± 0.82	0.80 ± 0.07	362 ± 54
DGEBA/BOX = 75/25 wt %	3250 ± 221	148 ± 15	6.41 ± 0.38	0.64 ± 0.08	214 ± 42
DGEBA/BOX = 50/50 wt %	3630 ± 108	147 ± 11	4.43 ± 0.58	0.69 ± 0.04	213 ± 21
DGEBA/BOX = 25/75 wt %	4655 ± 240	172 ± 19	3.75 ± 0.38	0.68 ± 0.03	210 ± 47
TGPAP-Ref	3498 ± 151	136 ± 13	5.37 ± 0.99	0.64 ± 0.04	162 ± 22
TGPAP/BOX = 75/25 wt %	3686 ± 109	155 ± 17	4.56 ± 0.74	0.74 ± 0.04	192 ± 9
TGPAP/BOX = 50/50 wt %	4225 ± 318	144 ± 25	3.47 ± 0.76	0.63 ± 0.03	145 ± 28
TGPAP/BOX = 25/75 wt %	4572 ± 82	151 ± 22	3.10 ± 0.49	0.67 ± 0.05	168 ± 20
TGDDM-Ref	3078 ± 149	126 ± 17	4.75 ± 0.97	0.63 ± 0.02	187 ± 13
TGDDM/BOX = 75/25 wt %	3700 ± 106	142 ± 35	4.04 ± 1.23	0.57 ± 0.03	150 ± 18
TGDDM/BOX = 50/50 wt %	4266 ± 126	185 ± 21	4.56 ± 0.85	0.61 ± 0.02	115 ± 8
TGDDM/BOX = 25/75 wt %	4630 ± 206	141 ± 21	2.82 ± 0.47	0.71 ± 0.05	176 ± 21

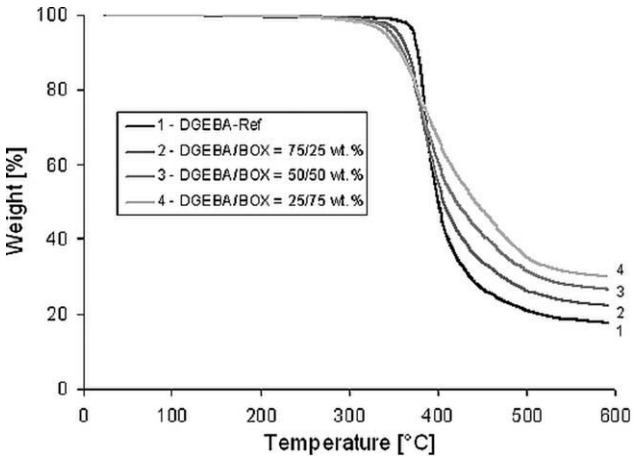

Figure 12 TGA traces registered for the DGEBA-Ref and DGEBA/BOX hybrids.

stoichiometry between EP and hardener caused by the appearance of phenolic —OH groups in the homopolymerized BOX.

Static flexure and fracture mechanical properties

The static flexural properties, that is, E-modulus (E_f), strength (σ_f) and displacement at maximum load (ε_f) are listed in Table II. One can establish that the E-modulus and flexure strength increased, whereas the displacement at maximum load decreased with increasing BOX content. This confirms that BOX acted as reinforcement in the related EP/BOX hybrids.

The fracture mechanical data, also listed in Table II, remain under expectation. Modification with BOX did not result in a clear trend in respect to the fracture toughness (K_c) and fracture energy (G_c). Both K_c and G_c were reduced by increasing BOX content for DGEBA/BOX, whereas practically no change in these fracture mechanical parameters could be noticed for the TGPAP/BOX and TGDDM/BOX systems.

TGA and fire resistance results

The TGA curves, registered on the DGEBA and DGEBA/BOX systems confirm that BOX incorporation improved the charring, see Figure 12. This was, however, not the case with TGPAP and TGDDM. Obviously, their thermal degradation behavior is controlled by the EP itself. The temperature values linked with 5 wt % loss ($T_{5\%}$), and the char yield at $T = 600°C$ are listed for all hybrids in Table I, too.

The flame resistance of the EP/BOX hybrids has been improved with increasing BOX content in all hybrids (cf. Table III). One can notice, however, that maximum V-1 classification could be reached. The data in Table III highlight that BOX hybridization was most successful for EP(DEGEBA) where V-1 was achieved already at DGEBA/BOX = 75/25 wt %.

CONCLUSIONS

Aromatic amine (DDM) curable EP resins of different functionalities were modified with BOX. The EP/DDM ratio was stoichiometric whereas the EP/BOX ratio was varied (EP/BOX = 100/0, 75/25, 50/50, and 25/75 wt %). BOX incorporation blurred the initial stoichiometry from which internal antiplasticization was expected. The morphology and various properties (thermal, thermomechanical, mechanical, and fire resistance) of the corresponding hybrids were determined and compared with those measured on the reference EPs. The outcome of this research work can be summarized as follows.

Network structure and morphology

The amine-hardened EP formed a conetwork with the BOX. The polymerized BOX appeared also in

TABLE III
UL-94 Flame Test Results for EP/BOX Hybrids

System	First ignition (s)	Dripping	Second ignition (s)	Dripping	Total combustion, 1st + 2nd = total, (s)	UL-94 class
DGEBA-Ref	35/87/31	No	10/0/10	No	153 + 20 = 173	Combustible
DGEBA/BOX = 75/25 wt %	28/25/18	No	8/9/11	No	71 + 28 = 99	V-1
DGEBA/BOX = 50/50 wt %	30/30/23	No	2/3/4	No	83 + 9 = 92	V-1
DGEBA/BOX = 25/75 wt %	30/22/16	No	0/3/2	No	68 + 5 = 73	V-1
TGPAP-Ref	33/54/83	Yes	10/6/0	No	170 + 16 = 186	Combustible
TGPAP/BOX = 75/25 wt %	54/21/36	Yes	3/7/5	No	111 + 15 = 126	Combustible
TGPAP/BOX = 50/50 wt %	9/44/36	No	15/6/12	No	89 + 33 = 122	Combustible
TGPAP/BOX = 25/75 wt %	11/30/12	No	12/0/0	No	53 + 12 = 65	V-1
TGDDM-Ref	29/29/86	Yes	40/46/0	Yes	144 + 86 = 230	Combustible
TGDDM/BOX = 75/25 wt %	71/52/13	Yes	2/6/12	No	136 + 20 = 156	Combustible
TGDDM/BOX = 50/50 wt %	30/15/23	No	4/6/12	No	68 + 22 = 90	V-1
TGDDM/BOX = 25/75 wt %	18/16/18	No	6/2/5	No	52 + 13 = 65	V-1

As only three specimens were tested, the related classification is of indicative character.

nanoscale inclusions in the EP. The dispersion characteristics of the most probably homopolymerized BOX depended on the EP functionality and EP/BOX ratio. The latter obviously influenced the curing-induced phase segregation of the homopolymerized BOX.

Mechanical properties

BOX incorporation enhanced the stiffness (E-modulus) and strength based on DMA and flexural tests. The polymerized BOX, present in homogenously copolymerized and phase separated homopolymerized forms, acted as efficient reinforcement in EP. However, none of the fracture mechanical parameters could be improved by adding BOX.

Thermal and fire resistance properties

The T_g of the hybrids was mostly lower than the reference EPs (especially for the trifunctional and tetrafunctional grades) that was traced to off-stoichiometry caused by the reactions between epoxy groups of the EP and phenolic —OH groups of the homopolymerized BOX. Incorporation of BOX increased the char yield only for the DGEBA/BOX system. According to UL94 V-1 classification could be reached with BOX hybridization.

Considering the fact that T_g was reduced and the modulus increased by BOX incorporation, the homopolymerized and copolymerized BOX acted as internal antiplasticizer in EP. The antiplasticizing effect was confirmed by changes in the β-relaxation of the EP that was influenced also by the γ-one of the polymerized BOX.

References

1. Reghunadhan Nair, C. P. Prog Polym Sci 2004, 29, 401.
2. Ghosh, N. N.; Kiskan, B.; Yagci, Y. Prog Polym Sci 2007, 32, 1344.
3. Yagci, Y.; Kiskan, B.; Ghosh, N. N. J Polym Sci Part A: Polym Chem 2009, 47, 5565.
4. Santhosh Kumar, K. S.; Reghunadhan Nair, C. P. Polybenzoxazines: Chemistry and Properties; Rapra: Shawbury, 2010.
5. Chernykh, A.; Agag, T.; Ishida, H. Polymer 2009, 50, 3153.
6. Gietl, T.; Lengsfeld, H.; Altstädt, V. J Mater Sci 2006, 41, 8226.
7. Ishida, H.; Allen, D. J Polym 1996, 37, 4487.
8. Rao, B. S.; Reddy, K. R.; Pathak, S. K.; Pasala, A. R. Polym Int 2005, 54, 1371.
9. Kimura, H.; Matsumoto, A.; Hasegawa, K.; Ohtsuka, K.; Fukuda, A. J Appl Polym Sci 1998, 1903, 68.
10. Kiskan, B.; Ghosh, N. N.; Yagci, Y. Polym Int 2011, 60, 167.
11. Agag, T.; Takeichi, T. High Perf Polym 2002, 14, 1.
12. Rimdusit, S.; Jongvisuttisun, P.; Jubsilp, C.; Tanthapanichaloon, W. J Appl Polym Sci 2009, 111, 1225.
13. Henkel Co. U.S. Pat. 2010/0099818 A1.
14. Rimdusit, S.; Ishida, H. J Polym Sci Part B: Polym Phys 2000, 38, 1687.
15. Kimura, H.; Matsumoto, A.; Ohtsuka, K. J Appl Polym Sci 2008, 109, 1248.
16. Grishchuk, S.; Mbhele, Z.; Schmitt, S.; Karger-Kocsis, J. Exp Polym Lett 2011, 5, 273.
17. Monsanto Co. U.S. Pat. 4,501,864 (1985).
18. Monsanto Co. U.S. Pat. 4,507,428 (1985).
19. Pascault, J.-P.; Sautereau, H.; Verdu, J.; Williams, J. J. J., Eds.; Thermosetting Polymers; Marcel Dekker: New York, 2002, p 334–336.
20. Available at: http://www.ides.com/property_descriptions/UL94. asp. Accessed on March 21, 2011 (IDES Inc.).
21. Nielsen, L. E. Mechanical Properties of Polymers and Composites; Marcel Dekker: New York, 1974, p 174–181.
22. Rao, B. S.; Pathak, S. K. J Appl Polym Sci 2006, 100, 3956.
23. Wirasate, S.; Dhumrongvaraporn, S.; Allen, D. J.; Ishida, H. J Appl Polym Sci 1998, 70, 1299.
24. Lin, H. T.; Lin, C. H.; Hu, Y. M.; Su, W. C. Polymer 2009, 50, 5685.
25. Heux, L.; Lauprêtre, F.; Halary, J. L.; Monnerie, L. Polymer 1998, 39, 1269.
26. Bershtein, V. A.; Peschanskaya, N. N.; Halary, J. L.; Monnerie, L. Polymer 1999, 40, 6687.
27. Chateauminois, A.; Sauvant, V.; Halary, J. L. Polym Int 2003, 52, 507.
28. Allen, D. J.; Ishida, H. J Appl Polym Sci 2006, 101, 2798.
29. Bellenger, V.; Dhaoui, W.; Verdu, J.; Boye, J.; Lacabanne, C. Polym Eng Sci 1990, 30, 321.
30. Boye, J.; Martinez, J. J.; Lacabanne, C. J Thermal Anal 1991, 37, 1775.
31. Palmese, G. R.; McCullough, R. L. J Appl Polym Sci 1992, 46, 1863.
32. Kosmidou, Th.; Vatalis, A. S.; Delides, C. G.; Logakis, E.; Pissis, P.; Papanicolaou, G. C. Exp Polym Lett 2008, 2, 364.
33. Rasoldier, N.; Colin, X.; Verdu, J.; Bocquet, M.; Olivier, L.; Chocinski-Arnault, L.; Lafarie-Frenot, M. C. Compos A 2008, 39, 1522.
34. Chocinski-Arnault, L.; Olivier, L.; Lafarie-Frenot, M. C. Mater Sci Eng A 2009, 521–522, 287.
35. Brostow, W.; Chonkaew, W.; Menard, K. P.; Scharf, T. W. Mater Sci Eng A 2009, 507, 241.
36. Colombini, D.; Martinez-Vega, J. J.; Merle, G. Polym Bull 2002, 48, 75.
37. Ning, X.; Ishida, H. J Polym Sci Part B: Polym Phys 1994, 32, 921.
38. Kim, H. J.; Brunovska, Z.; Ishida, H. J Appl Polym Sci 1999, 73, 857.
39. Burke, W. J.; Bishop, J. L.; Mortensen Glennie, E. L.; Bauer, W. N. J Org Chem 1965, 30, 3423.
40. Ishida, H.; Sanders, D. P. J Polym Sci Part B: Polym Phys 2000, 38, 3289.
41. Chutayothin, P.; Ishida, H. Macromolecules 2010, 43, 4562.
42. Santosh Kumar, K. S.; Reghunadhan Nair, C. P.; Ninan, K. N. Thermochim Acta 2006, 441, 150.
43. Crum, J. D.; Franks, J. A. J Heterocycl Chem 1965, 2, 37.
44. Daly, J.; Britten, A.; Garton, A.; McLean, P. D. J Appl Polym Sci 1984, 29, 1403.
45. Garton, A.; Mclean, P. D.; Stevenson, W. T. K.; Clark, J. N.; Daly, J. H. Polym Eng Sci 1987, 27, 1620.
46. Fink, J. K. In Fundamentals and applications: A concise guide to industrial polymers; William Andrew Publishing: Norwich, New York, 2005, Chapter 3, p 139–240.
47. Skourlis, T. P.; Mccullough, R. L. J Appl Polym Sci 1996, 62, 481.